Journal of Hazardous Materials Advances 3 (2021) 100014

Contents lists available at ScienceDirect

Journal of Hazardous Materials Advances

journal homepage: www.elsevier.com/locate/hazadv

Product analysis and insight into the mechanochemical destruction of anionic PFAS with potassium hydroxide

Mohamed Ateia*, Luke P. Skala, Anna Yang, William R Dichtel*

Department of Chemistry, Northwestern University, Evanston, Illinois, 60208, United States

ARTICLE INFO

Keywords:
Ball Milling
Per- and polyfluoroalkyl substances
Degradation efficiency
Co-milling reagents

ABSTRACT

Per- and polyfluoroalkyl substances (PFAS) are persistent, bioaccumulative, and potentially toxic chemicals that contaminate many water sources. Removing PFAS from water and ultimately degrading them into products that lack carbon-fluorine bonds will be important for decontaminating water resources. Among numerous emerging degradation methods, mechanochemical degradation of PFAS by ball milling has proven to be a simple and efficient method. However, the reaction pathway and final products after defluorination of PFAS have not been rigorously identified. Herein, we study anionic PFAS degradation by ball milling with alkali hydroxides and identify its degradation byproducts in the final powders for the first time. The degradation of PFAS occurred when KOH was used as a co-reagent, and no degradation is observed with LiOH, NaOH, and CsOH. Results showed degradation of both carboxylic and sulfonated PFAS within 24 h and best KOH:PFAS mass ratio was found to be approximately 20:1. Ion chromatography, thermogravimetric analysis, and ^{1}H, ^{13}C, and ^{19}F NMR spectroscopy revealed that milled powders obtained after perfluorocarboxylate degradation consisted of KF, K_2CO_3, and potassium formate. Perfluorinated sulfonates also produced K_2SO_4. Further, we characterized a byproduct by solid-state ^{19}F NMR spectroscopy that contains C_xF_x functional groups, which was formed during the degradation of all tested PFAS. The results and underlying methodology in this study will inform decisions on the scalability of ball milling processes for PFAS destruction, as well as the safe disposal of end products.

Introduction

Methods aimed at degrading of per- and polyfluoroalkyl substances (PFAS) in aqueous solutions include ultrasonication (Cheng et al., 2010), plasma (Singh et al., 2019), use of chemical oxidants such as persulfate (Hori et al., 2005; Parenky et al., 2020), ultraviolet-initiated degradation using additives such as sulfite (Bentel et al., 2020a; Bentel et al., 2020b; Bentel et al., 2019; Song et al., 2013) or iron (Liang et al., 2016), electrochemical degradation (Le et al., 2019; Schaefer et al., 2015), photocatalytic degradation (Qanbarzadeh et al., 2020; Sahu et al., 2018), and many other advanced oxidation and reduction techniques (Nzeribe et al., 2019). These techniques require large amounts of energy to break the C–F bonds in PFAS (Bentel et al., 2019). Further, some techniques have limited effectiveness because matrix effects decrease their efficiency in real water (Cheng et al., 2010; Liang et al., 2016), toxic byproducts can be generated through side reactions (Trautmann et al., 2015), and the low concentration of the PFAS in most waters requires high doses of chemical oxidants/reductants or energy inputs. Therefore, the treatment of PFAS-impacted waters will necessitate a treatment train approach. Previously tested tandem-mode setups consisted typically of a separation step (*e.g.*, activated carbon (Crimi et al., 2017; Watanabe et al., 2018), ion-exchange (IX) resin (Liang et al., 2018), biochar (Liu et al., 2019), or nanofiltration (Boonya-atichart et al., 2018; Soriano et al., 2017) followed by a destruction process applied to the adsorbents, retentate, and/or regeneration solutions. These methods include thermal mineralization (Watanabe et al., 2018), zerovalent iron (Boonya-atichart et al., 2018; Liu et al., 2019), electrochemical oxidation (Liang et al., 2018; Soriano et al., 2017), and activated persulfate (Crimi et al., 2017). However, current lab-scale and pilot-scale destruction methods could not address the full range of PFAS with different chain-length and functional groups (Nzeribe et al., 2019). In addition, incinerating PFAS adsorbed onto activated carbons is inefficient, requiring temperatures of 700–1000°C to induce PFAS mineralization (Watanabe et al., 2018; Watanabe et al., 2016; Xiao et al., 2020). Even at those conditions, studies suggest that volatile fluorocarbon greenhouse gases such as CF_4 or C_2F_6 are released during incineration (Shine and Sturges, 2007; Watanabe et al., 2018; Watanabe et al., 2016). In other cases, the incomplete incineration of PFAS-contaminated activated carbons has resulted in PFAS being discharged into the air and contaminating nearby communities.

The recent advancements in the development of PFAS-selective adsorbents (Ateia et al., 2019; Ching et al., 2020; Klemes et al., 2020),

* Corresponding authors.
E-mail addresses: mohamedateia1@gmail.com (M. Ateia), wdichtel@northwestern.edu (W.R. Dichtel).

https://doi.org/10.1016/j.hazadv.2021.100014
Received 14 July 2021; Received in revised form 23 September 2021; Accepted 2 October 2021

that are regenerable via a simple solvent wash, now offer the possibility of obtaining neat PFAS solids by evaporating the solvent in regeneration solutions. In addition, PFAS destruction has been reported using ball milling in the presence of co-reagents (e.g., potassium hydroxide, calcium oxide, alumina, sodium persulfate, zero-valent iron) (Cagnetta et al., 2016; Deng et al., 2020; Wang et al., 2019; Yan et al., 2015; Zhang et al., 2013). The milling is conducted in the solid phase, without solvents, at modest temperatures and pressures, which makes it well suited to destroy neat PFAS samples recovered from PFAS-selective adsorbents in a treatment train. The main advantage of this approach is that the end products are finely milled and environmentally innocuous inorganic salts (Cagnetta et al., 2016). Among tested co-reagents, KOH is a cheap and scalable option that showed efficient degradation of both carboxylic and sulfonic PFAS (Lu et al., 2017; Yan et al., 2015; Zhang et al., 2016; Zhang et al., 2013). Although degradation mechanisms have been proposed, the likely reaction pathway and even the final products of defluorination of PFAS have not been well studied (Cagnetta et al., 2016; Zhang et al., 2013). This understanding is essential to optimize the mechanochemical degradation conditions and identify byproducts, especially organofluorine compounds, that might present environmental or health concerns upon scale-up. Here we probe the degradation mechanisms and products of PFAS degradation when ball milled with KOH. By combining various spectroscopic techniques, we show that final milled solids consist of KF, K_2CO_3 and potassium formate for perfluorinated carboxylates, along with K_2SO_4 for perfluorosulfonates. Along with these major degradation products, we also discovered a byproduct formed upon ball milling of each PFAS that consists of molecules containing C_xF_x functional groups such as monofluorinated carbons or similar products (Krawietz and Haw, 1998). The findings of this research will inform decisions regarding scaling up mechanochemical PFAS destruction processes and the safe disposal of final products.

Materials and methods

Ball milling procedures

The ball mill used in this study was a planetary ball mill from MicroNano Tools, Ontario, Canada (Model: PBM-04) equipped with four 100 mL stainless steel grinding jars and stainless-steel balls. Each jar contained a mixture of 20 larger balls (9.6 mm) and 90 smaller balls (5.5 mm). The milling was performed by mixing PFAS powder with co-reagents as detailed in **Text S1**. After milling, 75 mL of either distilled (DI) water or methanol were added to the jar to characterize inorganic anions or PFAS, respectively. The different solvents were used because of the poor solubility of PFAS in DI water and insolubility of some target anions (*e.g.*, potassium sulfate and potassium bicarbonate) in methanol. All experiments were repeated three times using each solvent. The jars were then sonicated in a bath sonicator [BRANSON 3800, Frequency = 40 kHz] for 30 min before applying appropriate dilution of the solution in DI water for measuring PFAS and ion concentrations. The methanol-insoluble solids were analyzed after separating them by centrifugation and drying overnight at room temperature. Control samples were prepared following the same procedure without ball milling. We found that evaluating a portion of the solids after ball milling by dissolving a specific mass in a solvent provided inaccurate results and poor recovery of both PFAS and anions when compared to our methods that relied on dissolving the entire milled powder sample. We attribute this discrepancy to the false assumption that the total mass of the mixed materials is the same before and after milling, which does not account for mass losses (e.g., solid to gaseous products) and/or density changes after milling. Therefore, all analyses in the solid phase (e.g., FTIR or solid-state NMR spectroscopies) were performed on separate samples and were used for qualitative analysis only.

The solids recovered from the mechanochemical degradation experiments were analyzed using several measurements (**Text S2**), including liquid chromatography–mass spectrometry (LC-MS-MS), ion chromatography (IC), carbonate and bicarbonate measurement by titration, solution ^1H and ^{19}F nuclear magnetic resonance (NMR) spectroscopy in solution and the solid state, ^{19}F cross-polarization solid state NMR spectroscopy (CP-MAS), ^{13}C solid state NMR spectroscopy (ss-NMR), Fourier-transform infrared spectroscopy (FTIR), X-ray powder diffraction (XRD), and thermogravimetric analysis (TGA).

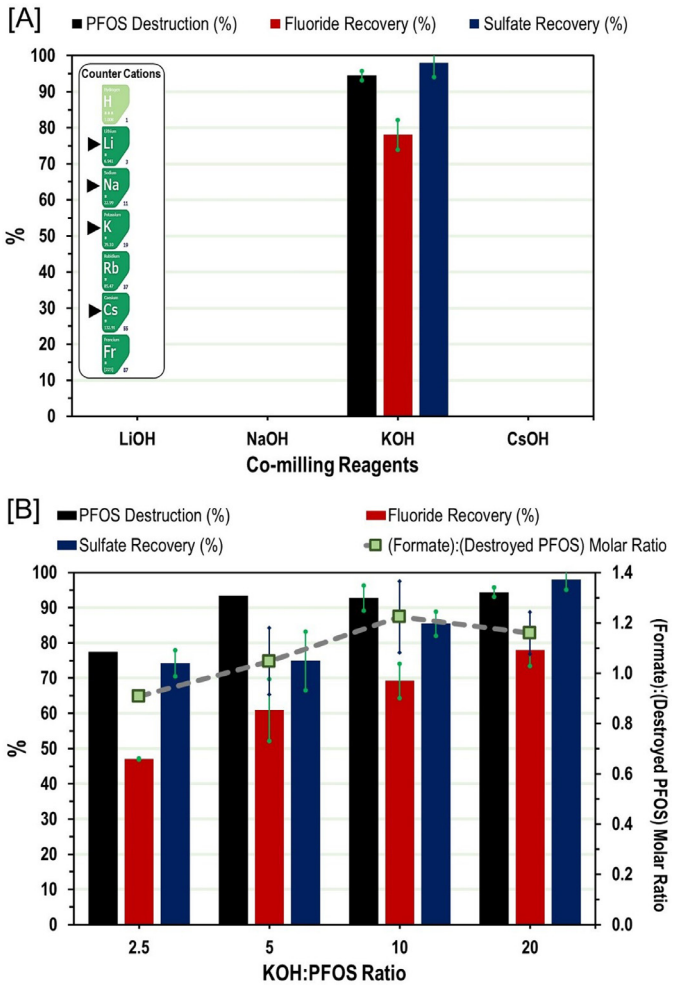

Fig. 1. [A] Testing LiOH, NaOH, KOH, and CsOH as co-reagents and the corresponding PFOS destruction, fluoride recovery and sulfate recovery. Co-reagent mass = 1g and PFAS mass = 50 mg. [B] Effects of increasing the mass ratio of KOH to PFOS on PFOS destruction, fluoride recovery, sulfate recovery, and formate formation. KOH mass was fixed at 1g and the ratio was varied by increasing PFOS concentrations from 50 to 400 mg. Vertical error bars show the standard deviation from triplicated experiments.

Results and discussion

LiOH, NaOH, KOH, and CsOH were tested as co-reagents for the mechanochemical degradation of PFOS. The degradation efficiency was tracked by measuring PFOS concentration by LC-MS-MS and the released fluoride and sulfate anions using IC. Only KOH showed destruction of PFOS and recovery of fluoride and sulfate anions, whereas no degradation was observed when the three other alkali hydroxides were used under the same conditions (**Fig. 1A**). These observations indicate that KOH has a unique mechanochemical activity from other alkali hydroxides. Although the exact differentiating property is unclear, the extreme conditions of localized high pressure and temperature during ball milling appear to favor KOH to initiate mechanochemical reactions that lead to C–F and C–C bond cleavage. To degrade PFAS using ball milling, bond-rupture processes occur via either mechanochemical reactions ac-

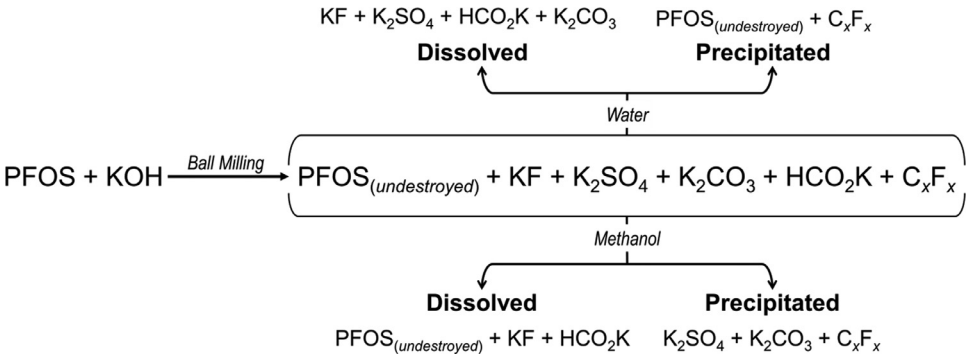

Scheme 1. XXX

tivated by deformation of valence bonds and angles under mechanical stress or via amorphization of the crystal structure (Dubinskaya, 1999). Zhang et al. (2013) reported that KOH degraded PFOS more readily than NaOH upon ball milling, however high fluoride ion recovery was observed only in the presence of KOH. These findings, combined with our observations that NaOH is incapable of PFOS degradation, are potentially explained by PFOS losses during PFOS collection and quantification in the previous report. Similarly, other reports have communicated conflicting findings on the effectiveness of other co-milling reagents. CaO was reported to be effective for PFOS degradation by Shintani et al. (2008), but showed only low activity in a later study by Zhang et al. (2013).

In kinetic experiments, a minimum of 20–24 h were required to achieve high recovery of anions and destruction of PFAS (**Figure S1**). This reaction time at 400 rpm was much longer than the reported 6–8 h at 275 rpm by Zhang et al. (2013), although it is unclear how milling times will translate from instrument to instrument (Cagnetta et al., 2016). The kinetics might also affected by the number and/or the mass of balls used in the reaction and their sizes, as well as the size and shapes of the milling jars (Boscoboinik et al., 2020; Broseghini et al., 2020). The key parameters that can cause these differences are either the milling intensity, which is the rate of energy transfer to the milled powders or the energy dose, which is the total amount of mechanical energy transferred to milled powder. These observations indicate that achieving the fastest and most efficient degradation may require re-optimization of the reaction time and rotational speed on a specific ball mill, especially as degradation processes are scaled. However, product analysis for these processes on small-scale instruments remains an important part of understanding these reactions.

The most extensive PFOS destruction, as evident by the high release of fluoride and sulfate anions, occurred under a KOH:PFOS mass ratio of ~20 under the tested operation conditions in this study (**Fig. 1B**). Therefore, the amount of KOH in the reaction controlled both the destruction of PFOS and the recovery of fluoride and sulfate, as demonstrated by the continuous increase of their values with increasing the mass ratio of KOH:PFOS. However, the molar ratios of the formate ion concentration to the destroyed PFAS, as measured by IC, were consistently 1.1 ± 0.1, regardless of tested conditions and targeted PFAS (**Fig. 1B and S2**). This molar ratio was consistent with formate concentration measured using ^{1}H NMR spectroscopy after 4 h and 24 h of milling time (**Figure S3**). This molar ratio indicates that only one carbon atom from the PFOS molecule is converted to formate. This ratio is inconsistent with a previously proposed "flake-off" degradation mechanism, in which PFAS would undergo a sequential chain-shortening by one CF_2 after decarboxylation or desulfonylation. Therefore, the flake-off mechanism should have generated one equivalent of formate per carbon found in the starting PFAS (Cagnetta et al., 2016). This finding represents a continued evolution in understanding the products and mechanism of mechanochemical PFAS destruction. In the first study by Zhang et al. (2013), formate was neither observed or proposed within the degradation pathway of PFOS and PFOA. However, formate was detected in later studies with other PFAS (Lu et al., 2017; Zhang et al., 2016), but its concentration was not quantified. These findings led to mechanistic proposals in which perfluoroalkyl carbons were eliminated from the PFAS compound as formate salts. Although this study proposed a different fragmentation pathway involving the elimination of perfluoropropyl fragments, whose carbons would subsequently be eliminated sequentially as formate ion (Cagnetta et al., 2016). Our consistent observations that each PFAS compound eliminates one molar equivalent of formate under these conditions is inconsistent with both of the above mechanisms and should cause other mechanisms to be probed. For now, it is not yet clear which carbon of each PFAS is converted into potassium formate.

Determining the components of complex mixtures in the milled powders necessitates measuring the same sample with multiple analytical techniques. For instance, previous studies used FTIR and XRD (Lu et al., 2017; Shintani et al., 2008), which showed low sensitivity to track the changes and to distinguish all transformations of milled chemicals (**Text S3 and Figures S4-S5**). Thus, we have employed ^{13}C ss-NMR for the first time and discovered that potassium carbonate, not potassium formate, is the major final product when KOH flakes were milled with either carboxylic or sulfonated PFAS (**Fig. 2**). Titration experiments to quantify carbonate in the milled powder further supported this finding with carbonate molar concentrations being 6–7 times higher than formate after milling of either PFOS or PFOA with KOH (**Figure S6**). TGA analysis of milled powders and their comparisons with standard salts (i.e., KOH, KF, K_2CO_3, $KHCO_3$, and K_2SO_4) have shown more evidence of such transformations including the increase in thermal stability of milled powders when compared to control samples without milling (**Text S3 and Figure S7**). TGA along with ion chromatography, ^{13}C ss-NMR, and solution NMR spectroscopy demonstrate that final milled powders consisted of potassium fluoride, potassium carbonate and potassium formate for carboxylic PFAS, as well as potassium sulfate for sulfonated PFAS. All of these inorganic salts are nontoxic and environmentally innocuous.

Evaluating the precipitated solids in methanol using ^{19}F ss-NMR also revealed an unexpected product of PFAS degradation. This product exhibited peaks in the region of –150 ppm to –250 ppm indicated that a minor degradation pathway results in the formation of a substance or substances containing C_xF_x functional groups. These products were observed for all tested PFAS (**Fig. 3 and S8**) (Arsenault et al., 2008). This is the first report of these degradation products for PFAS, which require more in-depth investigations to identify their structures and environmental fate. However, our current experimental data has shown the formed C_xF_x to be insoluble in all tested solvents in this study (i.e., water, methanol, DMSO, acetone, acetonitrile, and chloroform), which suggest the formation of CF_1 carbons or other similar stable final products (Krawietz and Haw, 1998). No short-chain PFAS was detected by LC-MS-MS after ball milling with KOH. Liquid ^{19}F NMR have also shown the decreased peak intensity of PFOA or PFOS and the emergence of KF with no other soluble fluorinated compounds (**Figures S9 and S10**).

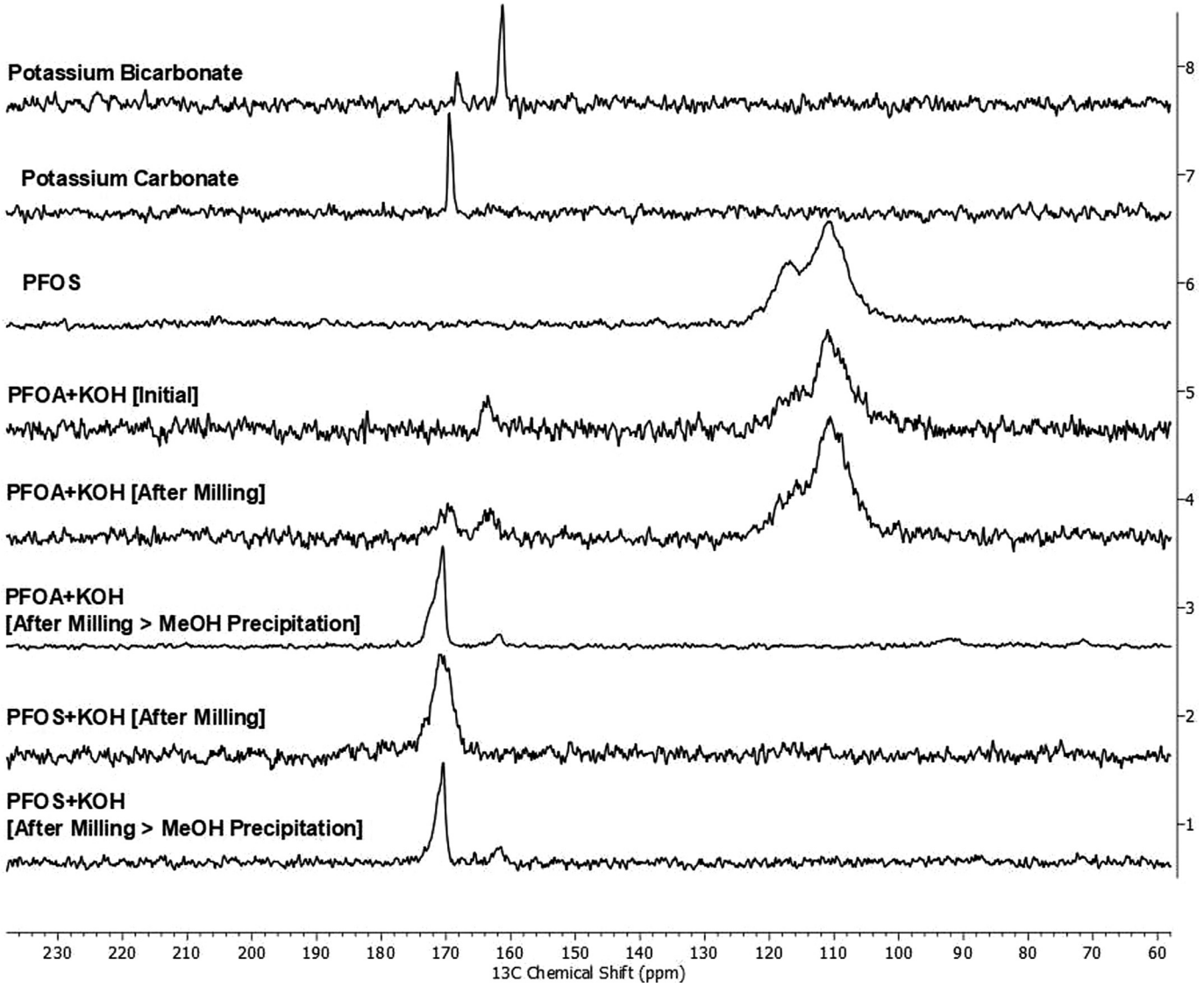

Fig. 2. ^{13}C ss-NMR spectra of PFOS and PFOA before and after ball milling with KOH for 24 h. MeOH precipitation was performed by adding methanol to milled powder and separating the precipitated solids by centrifugation and drying it at room temperature overnight.

Conclusions

Overall, Scheme 1 summarizes the reaction pathway according to our experimentally characterized degradation products. Except for the minor pathway that led to the formation of C_xF_x, the mineralization of PFAS to potassium salts appear to be rapid under the intense pressure and temperature during ball milling with KOH as co-reagent. These findings highlight the need to revisit the previously hypothesized degradation mechanisms of PFAS, which would require coupling mechanistic experiments and computational studies. Therefore, rigorous analysis of the energy transfer and reaction mechanisms are needed to cover the current knowledge gap about mechanochemical reactions. Unfolding the behavior of PFAS under mechanochemical stress will allow safe decisions on the scalability of the system and the fate of end products.

Associated content

Supporting Information Available. Test S1: Ball milling procedures and sample collection. Text S2: Analytical Procedures. Text S3: Results for FTIR, XRD, and TGA. Figures S1 to S10. This information is available free of charge on the ACS Publications website.

Notes

The authors declare the following competing financial interest(s): W.R.D owns equity and/or stock options in Cyclopure Inc., which partially funded this work and is commercializing PFAS adsorbents.

Statement of novelty

This research presents the first qualitative and quantitative identification of degradation products from the mechanochemical degradation of PFAS with KOH. Previously overlooked degradation products were tracked using ^{13}C and ^{19}F ss-NMR for the first time in addition to multiple other analytical techniques.

Declaration of Competing Interest

The authors declare that they have no known competing financial interests or personal relationships that could have appeared to influence the work reported in this paper.

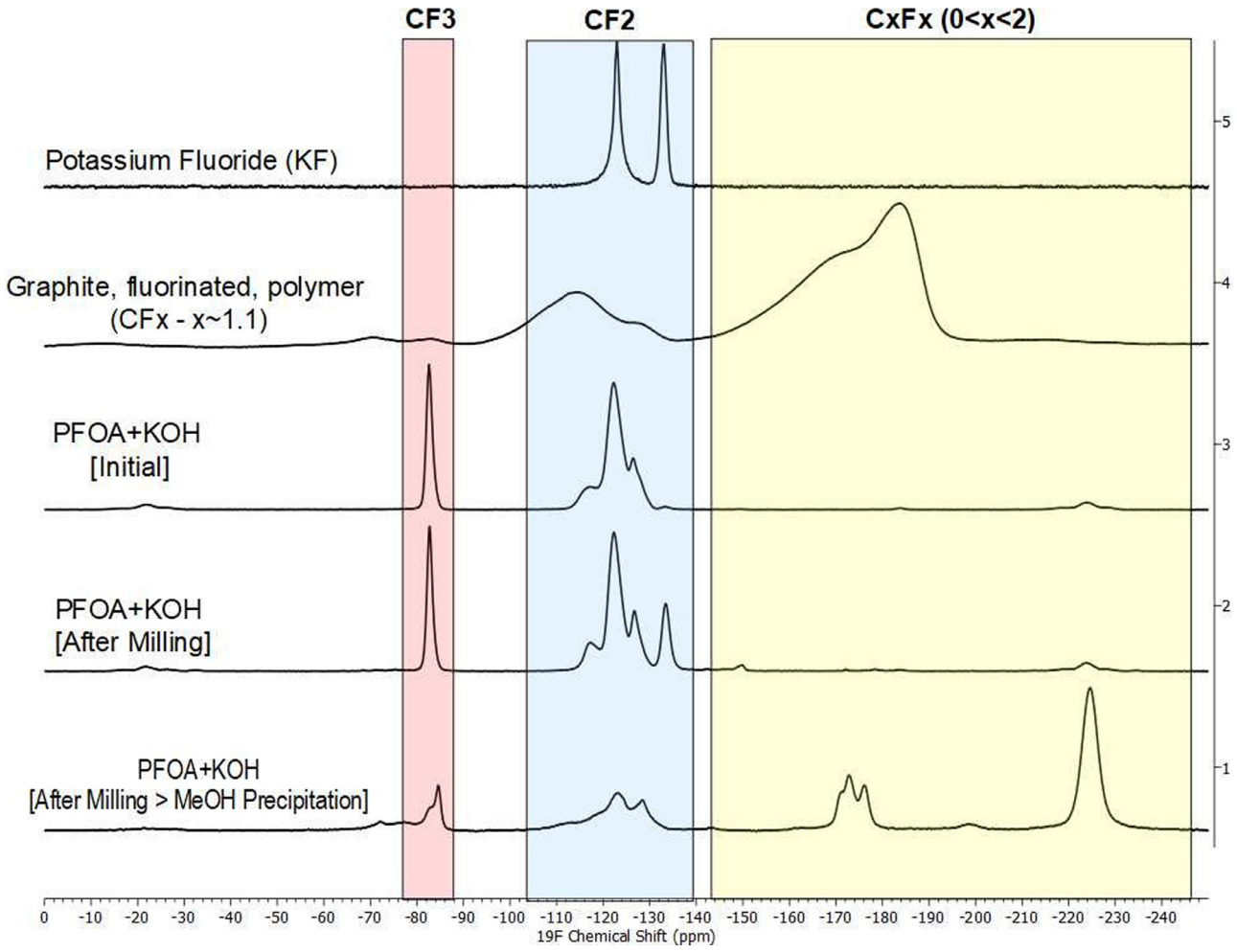

Fig. 3. ^{19}F ss-NMR spectra of PFOA before and after ball milling with KOH for 24 h. MeOH precipitation was performed by adding methanol to milled powder and separating the precipitated solids by centrifugation and drying it at room temperature overnight.

Acknowledgments

The study was partially supported by funding from Cyclopure Inc. Elemental analysis was performed at the Northwestern University Quantitative Bio-element Imaging Center. This work made use of the IMSERC NMR facility at Northwestern University, which has received support from the Soft and Hybrid Nanotechnology Experimental (SHyNE) Resource (NSF ECCS-2025633), Int. Institute of Nanotechnology, and Northwestern University.

L.P.S. is supported by the NSF Graduate Research Fellowship under grant DGE-1842165.

Supplementary materials

Supplementary material associated with this article can be found, in the online version, at doi:10.1016/j.hazadv.2021.100014.

References

Arsenault, G., Chittim, B., Gu, J., McAlees, A., McCrindle, R., Robertson, V., 2008. Separation and fluorine nuclear magnetic resonance spectroscopic (19F NMR) analysis of individual branched isomers present in technical perfluorooctanesulfonic acid (PFOS). Chemosphere 73 (1), S53–S59.

Ateia, M., Alsbaiee, A., Karanfil, T., Dichtel, W.R, 2019. Efficient PFAS removal by amine–functionalized sorbents: critical review of the current literature. Environ. Sci. Technol. Lett..

Bentel, M.J., Liu, Z., Yu, Y., Gao, J., Men, Y., Liu, J., 2020a. Enhanced degradation of perfluorocarboxylic acids (PFCAs) by UV/Sulfite treatment: reaction mechanisms and system efficiencies at pH 12. Environ. Sci. Technol. Lett. 7 (5), 351–357.

Bentel, M.J., Yu, Y., Xu, L., Kwon, H., Li, Z., Wong, B.M., Men, Y., Liu, J., 2020b. Degradation of perfluoroalkyl ether carboxylic acids with hydrated electrons: structure–reactivity relationships and environmental implications. Environ. Sci. Technol. 54 (4), 2489–2499.

Bentel, M.J., Yu, Y., Xu, L., Li, Z., Wong, B.M., Men, Y., Liu, J., 2019. Defluorination of per-and polyfluoroalkyl substances (PFASs) with hydrated electrons: structural dependence and implications to PFAS remediation and management. Environ. Sci. Technol. 53 (7), 3718–3728.

Boonya-atichart, A., Boontanon, S.K., Boontanon, N., 2018. Study of hybrid membrane filtration and photocatalysis for removal of perfluorooctanoic acid (PFOA) in groundwater. Water Sci. Technol. 2017 (2), 561–569.

Boscoboinik, A., Olson, D., Adams, H., Hopper, N., Tysoe, W.T., 2020. Measuring and modelling mechanochemical reaction kinetics. Chem. Commun. 56 (56), 7730–7733.

Broseghini, M., D'Incau, M., Gelisio, L., Pugno, N., Scardi, P, 2020. Numerical and experimental investigations on new jar designs for high efficiency planetary ball milling. Adv. Powder Technol. 31 (7), 2641–2649.

Cagnetta, G., Robertson, J., Huang, J., Zhang, K., Yu, G., 2016. Mechanochemical destruction of halogenated organic pollutants: a critical review. J. Hazard. Mater. 313, 85–102.

Cheng, J., Vecitis, C.D., Park, H., Mader, B.T., Hoffmann, M.R, 2010. Sonochemical degradation of perfluorooctane sulfonate (PFOS) and perfluorooctanoate (PFOA) in groundwater: kinetic effects of matrix inorganics. Environ. Sci. Technol. 44 (1), 445–450.

Ching, C., Klemes, M.J., Trang, B., Dichtel, W.R., Helbling, D.E, 2020. β-Cyclodextrin Polymers with Different Cross-Linkers and Ion-Exchange Resins Exhibit Variable Adsorption of Anionic, Zwitterionic, and Nonionic PFASs. Environ. Sci. Technol. 54 (19), 12693–12702.

Crimi, M., Holsen, T., Bellona, C., Divine, C., Dickenson, E., 2017. In situ treatment train for remediation of perfluoroalkyl contaminated groundwater. Situ Chemical Oxidation of Sorbed Contaminants (ISCO SC). Clarkson University Potsdam United States.

Deng, S., Bao, Y., Cagnetta, G., Huang, J., Yu, G., 2020. Mechanochemical degradation of perfluorohexane sulfonate: synergistic effect of ferrate (VI) and zero-valent iron. Environ. Pollut. 264, 114789.

Dubinskaya, A.M., 1999. Transformations of organic compounds under the action of mechanical stress. Russ. Chem. Rev. 68 (8), 637–652.

Hori, H., Yamamoto, A., Hayakawa, E., Taniyasu, S., Yamashita, N., Kutsuna, S., Kiatagawa, H., Arakawa, R., 2005. Efficient decomposition of environmentally persistent perfluorocarboxylic acids by use of persulfate as a photochemical oxidant. Environ. Sci. Technol. 39 (7), 2383–2388.

Klemes, M.J., Skala, L.P., Ateia, M., Trang, B., Helbling, D.E., Dichtel, W.R, 2020. Polymerized molecular receptors as adsorbents to remove micropollutants from water. Acc. Chem. Res. 190–194.

Krawietz, T., Haw, J., 1998. Characterization of poly (carbon monofluoride) by 19 F and 19 F to 13 C cross polarization MAS NMR spectroscopy. Chem. Commun. (19) 2151–2152.

Le, T.X.H., Haflich, H., Shah, A.D., Chaplin, B.P, 2019. Energy-efficient electrochemical oxidation of perfluoroalkyl substances using a Ti_4O_7 reactive electrochemical membrane anode. Environ. Sci. Technol. Lett. 6 (8), 504–510.

Liang, S., Pierce Jr, R.D., Lin, H., Chiang, S.Y., Huang, Q.J, 2018. Electrochemical oxidation of PFOA and PFOS in concentrated waste streams. Remediat. J. 28 (2), 127–134.

Liang, X., Cheng, J., Yang, C., Yang, S., 2016. Factors influencing aqueous perfluorooctanoic acid (PFOA) photodecomposition by VUV irradiation in the presence of ferric ions. Chem. Eng. J. 298, 291–299.

Liu, Y., Blowes, D.W., Ptacek, C.J., Groza, L.G, 2019. Removal of pharmaceutical compounds, artificial sweeteners, and perfluoroalkyl substances from water using a passive treatment system containing zero-valent iron and biochar. Sci. Total Environ. 691, 165–177.

Lu, M., Cagnetta, G., Zhang, K., Huang, J., Yu, G., 2017. Mechanochemical mineralization of “very persistent” fluorocarbon surfactants–6: 2 fluorotelomer sulfonate (6: 2FTS) as an example. Sci. Rep. 7 (1), 1–10.

Nzeribe, B.N., Crimi, M., Mededovic Thagard, S., Holsen, T.M, 2019. Physico-chemical processes for the treatment of per-and polyfluoroalkyl substances (PFAS): a review. Crit. Rev. Environ. Sci. Technol. 49 (10), 866–915.

Parenky, A.C., de Souza, N.G., Nguyen, H.H., Jeon, J., Choi, H., 2020. Decomposition of carboxylic PFAS by persulfate activated by silver under ambient conditions. J. Environ. Eng. 146 (10), 06020003.

Qanbarzadeh, M., Wang, D., Ateia, M., Sahu, S.P., Cates, E.L, 2020. Impacts of reactor configuration, degradation mechanisms, and water matrices on perfluorocarboxylic acid treatment efficiency by the UV/Bi3O (OH)(PO4) 2 photocatalytic process. ACS ES&T Eng. 1 (2), 239–248.

Sahu, S.P., Qanbarzadeh, M., Ateia, M., Torkzadeh, H., Maroli, A.S., Cates, E.L, 2018. Rapid degradation and mineralization of perfluorooctanoic acid by a new petitjeanite Bi_3O (OH)(PO_4) 2 microparticle ultraviolet photocatalyst. Environ. Sci. Technol. Lett. 5 (8), 533–538.

Schaefer, C.E., Andaya, C., Urtiaga, A., McKenzie, E.R., Higgins, C.P, 2015. Electrochemical treatment of perfluorooctanoic acid (PFOA) and perfluorooctane sulfonic acid (PFOS) in groundwater impacted by aqueous film forming foams (AFFFs). J. Hazard. Mater. 295, 170–175.

Shine, K.P., Sturges, W.T, 2007. CO2 is not the only gas. Science 315 (5820), 1804–1805.

Shintani, M., Naito, Y., Yamada, S., Nomura, Y., Zhou, S., Nakashimada, Y., Hosomi, M., 2008. Degradation of perfluorooctansulfonate (PFOS) and perfluorooctanoic acid (PFOA) by mechanochemical treatment. Kagaku Kogaku Ronbunshu 34 (5), 539–544.

Singh, R.K., Fernando, S., Baygi, S.F., Multari, N., Thagard, S.M., Holsen, T.M, 2019. Breakdown products from perfluorinated alkyl substances (PFAS) degradation in a plasma-based water treatment process. Environ. Sci. Technol. 53 (5), 2731–2738.

Song, Z., Tang, H., Wang, N., Zhu, L., 2013. Reductive defluorination of perfluorooctanoic acid by hydrated electrons in a sulfite-mediated UV photochemical system. J. Hazard. Mater. 262, 332–338.

Soriano, Á., Gorri, D., Urtiaga, A., 2017. Efficient treatment of perfluorohexanoic acid by nanofiltration followed by electrochemical degradation of the NF concentrate. Water Res. 112, 147–156.

Trautmann, A., Schell, H., Schmidt, K., Mangold, K.-M., Tiehm, A., 2015. Electrochemical degradation of perfluoroalkyl and polyfluoroalkyl substances (PFASs) in groundwater. Water Sci. Technol. 71 (10), 1569–1575.

Wang, N., Lv, H., Zhou, Y., Zhu, L., Hu, Y., Majima, T., Tang, H., 2019. Complete defluorination and mineralization of perfluorooctanoic acid by a mechanochemical method using alumina and persulfate. Environ. Sci. Technol. 53 (14), 8302–8313.

Watanabe, N., Takata, M., Takemine, S., Yamamoto, K., 2018. Thermal mineralization behavior of PFOA, PFHxA, and PFOS during reactivation of granular activated carbon (GAC) in nitrogen atmosphere. Environ. Sci. Pollut. Res. 25 (8), 7200–7205.

Watanabe, N., Takemine, S., Yamamoto, K., Haga, Y., Takata, M., 2016. Residual organic fluorinated compounds from thermal treatment of PFOA, PFHxA and PFOS adsorbed onto granular activated carbon (GAC). J. Mater. Cycles Waste Manage. 18 (4), 625–630.

Xiao, F., Sasi, P.C., Yao, B., Kubátová, A., Golovko, S.A., Golovko, M.Y., Soli, D., 2020. Thermal stability and decomposition of perfluoroalkyl substances on spent granular activated carbon. Environ. Sci. Technol. Lett. 7 (5), 343–350.

Yan, X., Liu, X., Qi, C., Wang, D., Lin, C., 2015. Mechanochemical destruction of a chlorinated polyfluorinated ether sulfonate (F-53B, a PFOS alternative) assisted by sodium persulfate. RSC Adv. 5 (104), 85785–85790.

Zhang, K., Cao, Z., Huang, J., Deng, S., Wang, B., Yu, G., 2016. Mechanochemical destruction of Chinese PFOS alternative F-53B. Chem. Eng. J. 286, 387–393.

Zhang, K., Huang, J., Yu, G., Zhang, Q., Deng, S., Wang, B., 2013. Destruction of perfluorooctane sulfonate (PFOS) and perfluorooctanoic acid (PFOA) by ball milling. Environ. Sci. Technol. 47 (12), 6471–6477.